Version for paper reading

Limits on contact interactions at HERA

ZEUS Collaboration

3rd December 2018

Abstract

The high-precision HERA data are used to set limits on possible high-energy "new physics" contributions to electron–quark scattering in the framework of *eeqq* contact interactions (CI). Combined measurements of the inclusive deep inelastic cross sections in neutral and charged current *ep* scattering are considered, corresponding to a luminosity of around 1 fb^{-1}. The analysis of the inclusive *ep* data is based on the simultaneous fits of parton distribution functions together with contributions of CI couplings to *ep* scattering. Different general CI models and scenarios with heavy leptoquarks are considered. Improvement in the description of the inclusive HERA data can be obtained for few models, corresponding to the CI mass scales in the few TeV range. However, more extensive theoretical studies on the Standard Model description of the HERA data are needed.

1 Introduction

The H1 and ZEUS collaborations measured inclusive $e^{\pm}p$ scattering cross sections at HERA from 1994 to 2000 (HERA I) and from 2002 to 2007 (HERA II), collecting together a total integrated luminosity of about $1\,\mathrm{fb}^{-1}$. All inclusive data were combined [1] to create one consistent set of neutral current (NC) and charged current (CC) cross-section measurements for $e^{\pm}p$ scattering with unpolarised beams. The inclusive cross sections were used as input to a QCD analysis within the DGLAP formalism, resulting in parton distribution function (PDF) parameterisations of the proton denoted as HERAPDF2.0. Precise knowledge of the parton densities inside the proton is crucial for the full exploitation of the physics potential of the LHC. In particular, when searching for possible beyond the Standard Model (BSM) effects, the parametrisation of the proton PDFs should not be biased by the possible BSM contributions.

HERA measurements of deep inelastic $e^{\pm}p$ scattering (DIS) cross sections at the highest values of negative four-momentum-transfer squared, Q^2, can be sensitive to BSM contributions even far beyond the centre-of-mass energy of the $e^{\pm}p$ interactions. For many "new physics" scenarios, cross sections can be affected by new kinds of interactions in which virtual BSM particles are exchanged. As the HERA kinematic range is assumed to be far below the scale of the new physics, all such BSM interactions can be approximated as contact interactions (CI).

The ZEUS collaboration has used the HERA combined measurement of inclusive cross sections [1] to set limits on possible deviations from the Standard Model (SM) due to a finite quark radius [2]. A new approach was used, based on the simultaneous fits of parton distribution functions together with contributions of "new physics" processes. This is the only method to properly take into account the possibility that the PDF set may already have been biased by partially or totally absorbing previously unrecognised BSM contributions. The intrinsic assumption remains that the original extraction of the cross sections from the raw data, which already involved Monte Carlos assuming the Standard Model, did not introduce a significant bias. This assumption is made for basically all analyses searching for "new physics". In the analysis presented here, the new procedure to set limits on the BSM model contributions introduced in [2] is extended to cover also other "new physics" scenarios. By including BSM contributions in the fit of parton distribution functions of the proton it is investigated whether the QCD evolution equations give the best possible description of the proton PDFs at highest Q^2, or if this description can be improved by including additional, non-standard terms.

2 Models for new physics

Four-fermion contact interactions (CI) represent an effective theory which describes low-energy effects due to physics at much higher energy scales. CI models describe the effects of heavy leptoquarks, additional heavy weak bosons and electron or quark compositeness. The CI approach is not renormalizable and is only valid in the low-energy limit. Vector contact interaction currents considered here are represented by additional terms in the SM Lagrangian:

$$\mathcal{L}_{\mathrm{CI}} = \sum_{\substack{i,j=L,R \\ q=u,d,s,c,b,t}} \eta_{ij}^{eq} (\bar{e}_i \gamma^\mu e_i)(\bar{q}_j \gamma_\mu q_j) \, , \tag{1}$$

where the sum runs over electron and quark chiralities and quark flavors. The couplings η_{ij}^{eq} describe the chiral and flavor structure of contact interactions.

Contrary to the SM expectations, the CI contribution to the electron–proton scattering amplitude does not depend on the energy scale of the process. In general, relative CI contribution to the DIS cross sections is therefore expected to be largest at the highest Q^2 values. However, the exact shape of the expected deviations from the SM predictions depends on the assumed flavour and chiral structure of the CI couplings. Depending on the coupling structure, different relations are also expected between electron–proton and positron–proton scattering contributions.

2.1 Contact interactions

For this study the contact interaction scenarios were defined as follows: it was assumed that all quarks have the same contact-interaction couplings,

$$\eta_{ij}^{eu} = \eta_{ij}^{ed} = \eta_{ij}^{es} = \eta_{ij}^{ec} = \eta_{ij}^{eb} = \eta_{ij}^{et} \, ,$$

leading to four independent couplings, η_{ij}^{eq}, with $i, j = L, R$. Due to the impracticality of setting limits in a four-dimensional space, a set of one-parameter scenarios was analysed. Each scenario is defined by a set of four coefficients, ϵ_{ij}, each of which may take the values ± 1 or zero, see Table 1, and the coupling strength η or compositeness scale Λ. The couplings are given by the formula:

$$\eta_{ij}^{eq} = \eta \, \epsilon_{ij} = \pm \frac{4\pi}{\Lambda^2} \epsilon_{ij} \, .$$

Selected for the presented study are four (parity violating) scenarios with defined coupling chirality, listed in the upper part of Table 1, and nine scenarios conserving parity (lower part of the table), for which the bounds resulting from atomic parity violation measurements can be avoided. Note that the coupling strength η can be both positive and negative, and the two cases are distinct because of the interference with the SM. Only in case of the VA model, the interference term contribution is negligible and the model predictions are mainly sensitive to η^2. When setting limits for BSM contributions, scenarios with positive and negative η values are considered separately.

2.2 Heavy leptoquarks

Leptoquarks (LQ) appear in certain extensions of the SM that connect leptons and quarks; they carry both lepton and baryon numbers and have spin 0 or 1. According to the general classification proposed by Buchmüller, Rückl and Wyler [3], there are 14 possible LQ states: seven scalar and seven vector[1]. In the limit of heavy LQs (for masses much higher than the HERA centre-of-mass energy, $M_{\mathrm{LQ}} \gg \sqrt{s}$), the effect of s- and t-channel LQ exchange is equivalent to a vector-type $eeqq$ contact interaction[2]. The effective LQ coupling, η_{LQ}, is given by the square of the ratio of the leptoquark Yukawa coupling, λ_{LQ}, to the leptoquark mass, M_{LQ}:

$$\eta_{\mathrm{LQ}} \;=\; \left(\frac{\lambda_{\mathrm{LQ}}}{M_{\mathrm{LQ}}}\right)^2 .$$

The contact-interaction couplings of the Lagrangian (1), η_{ij}^{eq}, can be then written as:

$$\eta_{ij}^{eq} \;=\; a_{ij}^{eq} \cdot \eta_{\mathrm{LQ}} \;=\; a_{ij}^{eq} \left(\frac{\lambda_{\mathrm{LQ}}}{M_{\mathrm{LQ}}}\right)^2 ,$$

where the coefficients a_{ij}^{eq} depend on the LQ species [6] and are twice as large for vector as for scalar leptoquarks. Only the positive values are allowed for the coupling η_{LQ} in the presented approach[3]. In the analysis presented in this paper, only the first-generation LQs are considered, $q = u, d$. Contrary to the considered CI scenarios, LQ coupling structure is different for u and d quarks, resulting also in different shape of the expected cross section deviations. The coupling structure for different leptoquark species is shown in Table 2.

[1] Leptoquark states are named according to the so-called Aachen notation [4].
[2] For the invariant mass range accessible at HERA, with $\sqrt{s} \sim 300\,\mathrm{GeV}$, the heavy LQ approximation is already applicable for $M_{\mathrm{LQ}} > 400\,\mathrm{GeV}$ [5].
[3] Note that five scalar and five vector LQ models correspond to the same coupling structure but with the opposite coupling sign for scalar and vector scenarios.

3 Extended fit to the inclusive HERA data

3.1 QCD+CI fit procedure

The analysis is based on a comparison of the measured inclusive cross sections with the model predictions. The effects of each CI scenario are taken into account by scaling the NLO QCD predictions at a given x, Q^2, corresponding to the inclusive cross section measurements [1], with the cross section ratio

$$R_{\mathrm{CI}} \;=\; \frac{\frac{d^2\sigma}{dx\,dQ^2}^{\mathrm{SM+CI}}}{\frac{d^2\sigma}{dx\,dQ^2}^{\mathrm{SM}}} \tag{2}$$

calculated in leading order (in electroweak and CI couplings[4]). As the CI contribution is expected to be small in the considered coupling range, possible higher order effects due to the cross section integration within x, Q^2 bins and to the use of standard QCD evolution in combination of HERA data are neglected.

The QCD analysis presented in this paper follows the approach adopted for the determination of HERAPDF2.0 [1]. This analysis is extended to take into account the possible BSM contributions to the expected cross section values, as described in a previous publication [2]. The PDFs of the proton are described at a starting scale of 1.9 GeV^2 in terms of 14 parameters. These parameters, denoted p_k in the following (or $\boldsymbol{p}$ for the set of parameters), together with the possible contribution of BSM phenomena (described by the CI coupling η) are fit to the data using a χ^2 method, with the χ^2 formula given by:

$$\chi^2\left(\boldsymbol{p}, \boldsymbol{s}, \eta\right) = \sum_i \frac{\left[m^i + \sum_j \gamma^i_j m^i s_j - \mu^i_0\right]^2}{\left(\delta^2_{i,\mathrm{stat}} + \delta^2_{i,\mathrm{uncor}}\right)\,(\mu^i_0)^2} + \sum_j s^2_j \quad . \tag{3}$$

Here μ^i_0 and m^i are the measured cross-section value and the SM+CI cross-section prediction at the point i. The quantities γ^i_j, $\delta_{i,\mathrm{stat}}$ and $\delta_{i,\mathrm{uncor}}$ are the relative correlated systematic, relative statistical and relative uncorrelated systematic uncertainties of the input data, respectively. The components s_j of the vector $\boldsymbol{s}$ represent the correlated systematic shifts of the cross sections (given in units of the respective correlated systematic uncertainties), which are fit to the data together with PDF parameter set $\boldsymbol{p}$ and the CI coupling η. The summations extend over all data points i and all correlated systematic uncertainties j.

The χ^2 formula used in this analysis was modified with respect to that of HERAPDF2.0 study [1]. The iterative procedure used to combine HERA data assures that the resulting

[4] Note that CIs constitute a non-renormalizable effective theory for which higher orders are not well defined.

cross section uncertainties are Gaussian. The χ^2 formula was changed to reflect the fact that we assume fixed Gaussian uncertainties of the input data points. The assumption that uncertainties are Gaussian is also used when generating the data replicas, see Section 4.

The resulting sets of PDFs, referred to as ZCIPDF in the following, are in very good agreement with HERAPDF2.0 fit results obtained within the HERAFitter framework [7]. The experimental uncertainties on the fitted model parameters and on the predictions from ZCIPDF, resulting from the uncertainties of the input HERA data, were defined by the criterion $\Delta\chi^2 = 1$. This takes into account statistical uncertainties but also correlated and uncorrelated systematic uncertainties of the combined HERA, see Eq. (3).

3.2 Modelling uncertainties

Following the approach used for the HERAPDF2.0 fit [1], the uncertainties on the ZCIPDF fit due to the choice of the form of the parameterisation and model settings were evaluated by varying the assumptions. A summary of the variations on model parameters is given in Table 3.

Two kinds of parameterisation uncertainties were considered, the variation in the fit starting scale, μ^2_{f0}, and the addition of parameters in the parton density parameterisation. The parameters D and E (see [1] for details) were added separately for each PDF. The final parameterisation uncertainty for a fit result is taken as the largest of the uncertainties.

The variations of charm and beauty mass parameters, M_c and M_b, respectively, were chosen in accordance with the mass estimation from HERAPDF2.0. The variation of the sea strange fraction, f_s, was chosen to span the ranges between a suppressed strange sea [8, 9] and an unsuppressed strange sea [10, 11]. In addition to these model variations, the minimal Q^2 of the data points used in the fit, $Q^2_{\rm min}$, was varied.

The differences between the central fit and the fits corresponding to the variations of $Q^2_{\rm min}$, f_s, M_c and M_b, and the largest parametrerisation uncertainty are added in quadrature, separately for positive and negative deviations, and represent the modelling uncertainty of the fit. The total PDF uncertainty is obtained by adding in quadrature the experimental and the modelling uncertainties.

3.3 Fit results

The QCD fit to the HERA inclusive data, corresponding to the ZCIPDF set of parton densities, was extended by adding the CI coupling, η (or $\eta_{\rm LQ}$ for LQ models) as the additional fit parameter. Results of the simultaneous QCD+CI fit to the HERA inclusive data, in terms of the fitted coupling values, are presented in Table 1 and Table 2, for contact interaction and heavy leptoquark scenarios, respectively. Experimental, modelling and total uncertainties on the fitted coupling values are calculated following the HERAPDF2.0 approach, as described above. Also shown is the change of the χ^2 value from the nominal SM fit, $\Delta\chi^2 = \chi^2 - \chi^2_{\mathrm{SM}}$. For most of the considered CI scenarios only one minimum is observed in the χ^2 dependence on the coupling value. Only in case of the VA model two minima are observed in the χ^2 function, one for positive and one for negative couplings. Results for both minima are presented in Table 1.

In most cases correlations between PDF parameters and CI coupling values resulting from the QCD+CI fit are small. The largest correlation are observed between the CI coupling and parameters B_{d_v}, B_{u_v} and $C_{\bar{D}}$, used in the description of the valence d quark, valence u quark and d-type anti-quark distribution, respectively. Their absolute values reach up 0.61 for CI models ($\eta - B_{d_v}$ correlation in AA model) and 0.57 for LQ models ($\eta - C_{\bar{D}}$ correlation in V_0^L model).

For six considered CI scenarios (out of 13) and seven heavy leptoquark models (out of 14) no significant improvement in the data description is observed (consistent with $\Delta\chi^2 \approx -1$ expected for number of degrees of freedom reduced by one) and the fitted coupling values for these models are consistent with zero (in agreement with SM predictions). However, there are also four models (three CI and one[5] LQ scenario), which result in an improved description of the data, with $\Delta\chi^2 < -4$. The best description of the inclusive HERA data is obtained for the X6 contact interaction model ($\Delta\chi^2 = -6.01$) and S_1^L heavy leptoquark model ($\Delta\chi^2 = -11.10$). The fit results for these models are compared with HERA NC DIS data in Fig. 1 and Fig. 2, respectively. Also indicated is the SM contribution to the NC DIS cross sections obtained from the QCD+CI fit.

For the X6 model, the determination of the proton PDFs is hardly affected by the CI contribution. The SM part of the NC DIS cross sections extracted from the QCD+CI fit agree with the nominal ZCIPDF fit within the quoted PDF uncertainties. The deviation observed in the NC DIS cross section is dominated by the CI contribution. The situation is different for the S_1^L heavy leptoquark model. The description of the parton densities in the proton is significantly affected when the heavy LQ contribution is taken into account in the fit. The cross section for NC e^+p DIS with γ/Z° exchange increases at the highest values of Q^2, $Q^2 > 50\,000\,\mathrm{GeV}^2$, by about a factor of two. The virtual leptoquark exchange contribution to the NC e^+p DIS cross section is much smaller than the change observed in the SM contribution. Moreover, it decreases the total cross section due to the negative interference with the SM part. The improvement in the inclusive data description for the S_1^L heavy leptoquark model is also due to the better agreement with the CC DIS data.

Table 1 includes also estimates of the modelling (and the resulting total) uncertainties on the fitted CI coupling values. For most models modelling uncertainties tend to be small, below the level of experimental uncertainties. However, they turn out to be significant for

[5] The improvement observed for the V_0^L model is not considered, as it is obtained for unphysical (negative) coupling value.

the three CI models (AA, X1 and X6) for which possible deviations from SM predictions were observed. The largest fit result variations for these models are observed due to the choice of the $Q^2_{\rm min}$ parameter (used to select input data set for the fit) and when including an additional parameter in the valence u-quark density description. In particular, when the functional form used to describe the u-quark density is modified (adding parameter D_{u_v} [1]), the χ^2 value from the SM fit to the data is reduced by $\Delta\chi^2 = -10.3$. At the same time the CI coupling values resulting from the QCD+CI fit, $\eta^{\rm Data}$, decrease (in the absolute value). The improvement due to the additional CI contribution becomes much less pronounced, with $\Delta\chi^2 > -2$ for the three considered models.

The situation is different for the S_1^L leptoquark scenario. Although modelling uncertainties are sizeable, see Table 2, they can not explain the significant in the description of the HERA data when adding the S_1^L leptoquark exchange contribution to the fit. The QCD+CI fit results in $\Delta\chi^2 < -9$ for all considered model and parameterisation variations. For the S_1^L leptoquark scenario the NC e^-p DIS cross section is enhanced at the highest Q^2 values, while for the e^+p scattering the enhancement is rather expected at large x values[6]. A cross-check was also made using the bilog parameterisation. While the overall description achieved with this quite different ansatz is much worse than than the description achieved with HERAPDF parameterisation, an S_1^L term of similar strength is found.

4 Statistical analysis

4.1 Data set replicas

To estimate the statistical significance of the differences from the SM predictions indicated by the fit results presented in Section 3.3, the technique of the so called replicas is used. Replicas are sets of cross-section values, corresponding to the HERA inclusive data set, that are generated by varying all cross sections randomly according to their known uncertainties. For the analysis presented here, multiple replica sets were used, each covering cross-section values on all points of the x, Q^2 grid used in the QCD fit. For an assumed true value of the CI coupling, $\eta^{\rm True}$, replica data sets were created by taking the reduced cross sections calculated from the nominal PDF fit (with CI coupling $\eta \equiv 0$) and scaling them with the cross section ratio $R^{\rm CI}$ given by Eq. 2. This results in a set of cross-section values m_0^i for the assumed true CI coupling $\eta^{\rm True}$. The values of m_0^i were then varied randomly within statistical and systematic uncertainties taken from the data, taking correlations of systematic uncertainties into account. All uncertainties were assumed to follow a Gaussian

[6] This is due to an additional kinematic factor of $(1-y)^2$ multiplying the LL scattering amplitude for NC e^+p DIS.

distribution[7]. For each replica, the generated value of the cross section at the point i, μ^i, was calculated as:

$$\mu^i = \left[m_0^i + \sqrt{\delta^2_{i,\mathrm{stat}} + \delta^2_{i,\mathrm{uncor}}} \cdot \mu_0^i \cdot r_i\right] \cdot \left(1 + \sum_j \gamma_j^i \cdot r_j\right) \quad , \tag{4}$$

where variables r_i and r_j represent random numbers from a normal distribution for each data point i and for each source of correlated systematic uncertainty j, respectively.

The adopted approach was to generate large sets of replicas and use them to test the hypothesis that the cross sections are consistent with the SM predictions or that they were modified by a fixed CI coupling according to Eq. 2. The value of η^{Data} determined by the fit to the data themselves was taken as a test statistic, to which values from fits to replicas, η^{Fit}, could be compared.

To quantify the statistical consistency of the fit results with the SM expectations, the probability that an experiment assuming validity of the SM (replicas generated with $\eta^{\mathrm{True}} = \eta^{\mathrm{SM}} = 0$) would produce a value of η^{Fit} greater than (or less than) that obtained from the data is calculated:

$$p_{\mathrm{SM}} = \begin{cases} p(\eta^{\mathrm{Fit}} > \eta^{\mathrm{Data}}) & \text{for} \quad \eta^{\mathrm{Data}} > 0 \, , \\ p(\eta^{\mathrm{Fit}} < \eta^{\mathrm{Data}}) & \text{for} \quad \eta^{\mathrm{Data}} < 0 \, , \end{cases} \tag{5}$$

where probability p is calculated from the distribution of η^{Fit} values for a large set of generated SM replicas.

4.2 Constraining BSM scenarios

The technique of replicas described above can be also used to calculate the coupling limits for the considered CI scenarios and the corresponding mass scale limits in a frequentist approach [12]. As mentioned in Section 2.1, in case of the CI scenarios coupling limits are calculated separately for positive and negative η values. The upper (lower) 95% C.L. limit on positive (negative) coupling, η^+ (η^-), for a given scenario is determined as the value of η^{True} at which 95% of the replicas produce a fitted coupling value, η^{Fit}, larger (lower) than that found in the data. The corresponding mass scale values (Λ^+ and Λ^- for CI scenarios or M/λ for LQ models) will be refered to as mass scale limits.

A similar procedure is also used to calculate the expected limit values, which are defined by comparing replica fit results with $\eta^{\mathrm{SM}} \equiv 0$ instead of η^{Data}. The details of these procedures are described in [2].

[7] It was verified that using a Poisson probability distribution for producing replicas at high Q^2, where the event samples are small, and using the χ^2 minimisation for these data did not significantly change the probability distributions for the fitted parameter values.

To take modelling uncertainties into account the limit calculation procedure is repeated for model or parameterisation variations resulting in highest and lowest η^{Data} values for each model. The weakest of the obtained coupling limits is taken as the result of the analysis and used to calculate the final mass scale limits. This is clearly the most conservative approach, which is however motivated by the difficulty in defining the underlying probability distribution for some of the considered modelling variations.

The dependence of the coupling limits on the modelling variations reflects mainly the changing fit results (η^{Data} values). As the expected limits do not depend on η^{Data} (replica fit results are compared to $\eta^{\mathrm{SM}} \equiv 0$) they are hardly sensitive to the modelling variations. Therefore, these variations are not considered for the expected limits.

At least 3000 Monte Carlo replicas had to be generated and fitted for each value of η^{True} and for each considered CI or LQ scenario. When using xFitter to perform replica fits processing time was a limiting factor for including more models in the analysis. To facilitate efficient processing of replica data, a simplified fit method, based on the Taylor expansion of the cross section predictions in terms of PDF parameters was developed, which reduced the calculation time by almost two orders of magnitude [13].

5 Results

The probabilities p_{SM} (Eq. (5)) calculated for the considered CI scenarios with the SM replica sets are presented in Table 4. Statistical approach based on Monte Carlo replicas confirms the observations described in Section 3.3, based on the $\Delta\chi^2$ values. For six CI models (LR, RL, VV, X2, X4 and X5) p_{SM} is above 20%, corresponding to less than 1σ deviation from the nominal fit result ($\eta^{\mathrm{Fit}} = \eta^{\mathrm{SM}} = 0$). For another four models (LL,LR, VA and X3), data fit results are reproduced by the SM replicas with 3–7% probability, corresponding to about 2σ difference. However, for three scenarios (AA, X1 and X6) with $\Delta\chi^2 < -4$, p_{SM} is below 1%. This confirms that the discrepancies between the HERA data and the SM predictions described by the additional CI contribution in the fit are not likely to be due to the statistical fluctuations only. As already discussed in Section 3.3, the effect can be explained to some extent by the modelling uncertainties, in particular by the deficiencies in the functional form used for the PDF parametrisation.

Also shown in Table 4 are the 95% C.L. limits on the coupling values, η^- and η^+, for different CI models. Limits calculated without (exp) and with (exp+mod) taking into account model and parameterisation variations, as described above, are compared with expected coupling limits in Fig. 3. The coupling limits can also be translated into the limits on the compositeness scales for the considered CI scenarios, also included in Table 4.

For most of the considered CI scenarios the interference term gives a significant contribution to the cross section and the sign of the CI coupling is well constrained in the fit.

However, in case of the VA model the contribution from the interference term is much smaller than the direct CI contribution proportional to the coupling squared. As a result, the model predictions are hardly sensitive to the coupling sign and the global minima of the χ^2 function is often observed for the "wrong" coupling sign (i.e. different from that of η^{True}). The limits on the CI coupling, calculated using the procedure described above, are therefore very weak ($\eta^- = -4.4\,\mathrm{TeV}^{-2}$ and $\eta^+ = 2.5\,\mathrm{TeV}^{-2}$). To solve this problems, we calculate limits for the VA model, restricting the fit range to negative or positive couplings, for lower and upper coupling limit respectively.

Compositeness scale limits calculated taking modelling uncertainties into account range from 3.1 TeV for X6 model (Λ^-) up to 17.9 TeV for the X3 model (Λ^-). For the three models mentioned above (AA, X1 and X6), when only experimental uncertainties are considered, one sign of CI coupling is excluded at 95% C.L. and the limit for the coupling and compositeness scale Λ are presented only for the other sign. The effect persists for X1 and X6 scenarios also when modelling uncertainties are taken into account. In Fig. 5, the measured Q^2 spectra for e^+p and e^-p combined HERA data, relative to the SM predictions calculated using the HERAPDF2.0 parameterisation, are compared with the expectations for VV and AA contact-interaction models which correspond to the compositeness limits described above.

The LQ coupling values determined from the fit to the HERA inclusive data, $\eta_{\mathrm{LQ}}^{\mathrm{Data}}$ and probabilities p_{SM} are summarized in Table 5 together with the coefficients a_{ij}^{eq} describing the CI coupling structure of the considered LQ models. Also shown are the 95% C.L. upper limits on the ratio of the Yukawa coupling to the leptoquark mass, $\lambda_{\mathrm{LQ}}/M_{\mathrm{LQ}}$. Limits calculated without (exp) and with (exp+mod) taking into account model and parameterisation variations are compared with the expected 95% C.L. limits on $\lambda_{\mathrm{LQ}}/M_{\mathrm{LQ}}$ in Fig. 4.

For S_1^L model, improvement in the description of HERA data can be obtained and probability of reproducing the fit result with Standard Model replicas, p_{SM}, is below 0.01%. Also for the V_0^R model, the probability p_{SM} is below 5%, which means that $\eta_{\mathrm{LQ}} = 0$ (corresponding to the Standard Model) is excluded for this scenario ($p_{\mathrm{SM}} = 1.8\%$), when only experimental uncertainties are taken into account. When modelling uncertainties are taken into account, the corresponding p_{SM} values increase, but SM is still outside the allowed range for both models.

Also for $\tilde{S}_0^R$ and V_0^L models[8] a probability below 5% is obtained, but the fit points to unphysical (negative) coupling values and both models are excluded on 95% C.L.

Assuming the Yukawa coupling value, $\lambda_{\mathrm{LQ}} = 1$, the corresponding lower limits on the leptoquark mass range from 0.66 TeV for the $\tilde{S}_{1/2}^L$ model to 16 TeV for the $\tilde{V}_0^R$ model. When modelling uncertainties are included, the limits range from 0.60 TeV to 5.6 TeV. Deviations in the Q^2 distribution of e^+p and e^-p NC DIS events, corresponding to the

[8] Note that the $\tilde{S}_0^R$ is related to the V_0^R model, corresponding to the same CI coupling structure, but with different sign. The fit results are therefore not independent.

95% C.L. coupling limits for S_1^L and V_0^R leptoquark models, are compared with HERA data in Fig. 6.

Comparison of presented results with limits obtained by CMS [14] and ATLAS [15] experiments at LHC, based on the data collected at 8 TeV and 13 TeV, respectively, is presented in Table 6. Only the four presented CI models were considered in the analysis of the LHC data. It is clear that the statistical sensitivity of the LHC experiments, in particular when using the 13 TeV data, is much higher than of the HERA inclusive data. However, the systematic uncertainties resulting from the proton PDFs can be underestimated, as the possible bias in the parameterisation was not taken into account.

6 Conclusions

The HERA combined measurement of inclusive deep inelastic cross sections in neutral and charged current $e^{\pm}p$ scattering was used to search for possible deviations from the Standard Model predictions within the *eeqq* contact interaction approximation. The procedure was based on a simultaneous fit of PDF parameters and the CI coupling. Confidence intervals on the CI couplings and p-values for the SM predictions were obtained with Monte Carlo replicas. Limits on the effective CI mass scales, Λ, and limits on the ratio of the leptoquark Yukawa coupling to the leptoquark mass, $\lambda_{\mathrm{LQ}}/M_{\mathrm{LQ}}$, corresponding to the coupling intervals resulting from the replica analysis were also calculated, with and without taking into account modelling uncertainties in the QCD fit procedure.

For AA, VA, X1 and X6 models, SM+CI predictions give an improved description of the HERA inclusive data, corresponding to the deviation from the SM predictions at the level of up to 2.7 σ (SM probability of 0.3% for X6 model). This is unlikely to be explained by statistical fluctuations only, but can be partially explained by the modelling uncertainties in the fitting procedure. A similar effect is observed for S_1^L and V_0^R leptoquark models, which give improved description of HERA inclusive data, corresponding to the deviation from the SM predictions at the level of about 4 σ and about 2 σ, respectively. In particular, the fits suggest the positive deviation in NC e^-p DIS at highest Q^2. For the S_1^L model the discrepancy is most significant and is unlikely to be explained by any of the considered model on parameterisation variations. This indicates that theoretical description of the parton densities evolution in the proton or of the electron–proton DIS at highest Q^2 need to be improved. Theoretical predictions have to be reexamined carefully and possible contributions of higher-order effects have to be estimated before the observation can be attributed to any scenario of "new physics". In spite of the difficulties in modeling the DIS data, limits in the TeV mass range for some of the contact interactions have been achieved.

References

[1] H1 and ZEUS Collaborations, H. Abramowicz et al., Combination of Measurements of Inclusive Deep Inelastic $e^{\pm}p$ Scattering Cross Sections and QCD Analysis of HERA Data, Eur. Phys. J. **C 75**, 580 (2015). doi:10.1140/epjc/s10052-015-3710-4. `arXiv:1506.0604`.

[2] ZEUS Collaboration, H. Abramowicz et al., Limits on the effective quark radius from inclusive ep scattering at HERA, Phys. Lett. **B757**, 468 (2016). doi:10.1016/j.physletb.2016.04.007. `arXiv:1604.0128`.

[3] W. Buchmüller, R. Rückl and D. Wyler, Leptoquarks in lepton–quark collisions, Phys. Lett. **B 191**, 442 (1987). doi:10.1016/0370-2693(87)90637-X. Erratum in Phys. Lett. **B 448**, 320 (1999). doi:10.1016/S0370-2693(99)00014-3.

[4] A. Djouadi et al., (eb)-, (et)-type leptoquarks at ep-colliders, Z. Phys. **C 46**, 679 (1990). doi:10.1007/BF01560270.

[5] ZEUS Collaboration, H. Abramowicz et al., Search for first-generation leptoquarks at HERA, Phys. Rev. **D86**, 012005 (2012). doi:10.1103/PhysRevD.86.012005. `arXiv:1205.5179`.

[6] J. Kalinowski et al., Leptoquark/squark interpretation of HERA events: Virtual effects in e^+e^- annihilation to hadrons, Z. Phys. **C 74**, 595 (1997). doi:10.1007/s002880050424. `arXiv:hep-ph/9703288`.

[7] S. Alekhin et al., HERAFitter, Eur. Phys. J. **C75**, 304 (2015). doi:10.1140/epjc/s10052-015-3480-z. `arXiv:1410.4412`.

[8] A.D. Martin, W.J. Stirling, R.S. Thorne and G. Watt, Parton distributions for the LHC, Eur. Phys. J. **C63**, 189 (2009). doi:10.1140/epjc/s10052-009-1072-5. `arXiv:0901.0002`.

[9] P.M. Nadolsky, H.-L. Lai, Q.-H. Cao, J. Huston, J. Pumplin, D. Stump, W.-K. Tung and C.-P. Yuan, Implications of CTEQ global analysis for collider observables, Phys. Rev. **D78**, 013004 (2008). doi:10.1103/PhysRevD.78.013004. `arXiv:0802.0007`.

[10] ATLAS Collaboration, G. Aad et al., Determination of the strange quark density of the proton from ATLAS measurements of the $W \to \ell\nu$ and $Z \to \ell\ell$ cross sections, Phys. Rev. Lett. **109**, 012001 (2012). doi:10.1103/PhysRevLett.109.012001. `arXiv:1203.4051`.

[11] ATLAS Collaboration, M. Aaboud et al., Precision measurement and interpretation of inclusive W^+ , W^- and Z/γ^* production cross sections with the ATLAS detector, Eur. Phys. J. **C77**, 367 (2017). doi:10.1140/epjc/s10052-017-4911-9. `arXiv:1612.0301`.

[12] R.D. Cousins, Why isn't every physicist a Bayesian?, Am. J. Phys. **63**, 398 (1995).

[13] O. Turkot, K. Wichmann and A.F.Zarnecki, Simplified QCD fit method for BSM analysis of HERA data, 2016.

[14] CMS Collaboration, V. Khachatryan et al., Search for physics beyond the standard model in dilepton mass spectra in proton-proton collisions at $\sqrt{s} = 8$ TeV, JHEP **04**, 025 (2015). doi:10.1007/JHEP04(2015)025. `arXiv:1412.6302`.

[15] ATLAS Collaboration, M. Aaboud et al., Search for new high-mass phenomena in the dilepton final state using 36 fb^{1} of proton-proton collision data at $\sqrt{s} = 13$ TeV with the ATLAS detector, JHEP **10**, 182 (2017). doi:10.1007/JHEP10(2017)182. `arXiv:1707.0242`.

ZEUS

HERA $e^{\pm}p$ 1994-2007 data

Coupling structure		Coupling fit results (TeV^{-2})				$\Delta\chi^2$
Model	$[\epsilon_{LL},\ \epsilon_{LR},\ \epsilon_{RL},\epsilon_{RR}]$	η^{Data}	δ_{exp}	δ_{mod}	δ_{tot}	
LL	$[+1,\ 0,\ 0,\ 0]$	0.305	0.206	$^{+0.017}_{-0.037}$	$^{+0.207}_{-0.209}$	−2.06
RR	$[\ 0,\ 0,\ 0,+1]$	0.338	0.210	$^{+0.019}_{-0.038}$	$^{+0.210}_{-0.213}$	−2.30
LR	$[\ 0,\ +1,\ 0,\ 0]$	−0.084	0.247	$^{+0.212}_{-0.060}$	$^{+0.325}_{-0.254}$	−0.12
RL	$[\ 0,\ 0,\ +1,\ 0]$	−0.040	0.241	$^{+0.198}_{-0.057}$	$^{+0.312}_{-0.248}$	−0.03
VV	$[+1,\ +1,\ +1,+1]$	0.041	0.061	$^{+0.024}_{-0.009}$	$^{+0.066}_{-0.062}$	−0.45
AA	$[+1,\ -1,\ -1,+1]$	0.326	0.161	$^{+0.250}_{-0.175}$	$^{+0.297}_{-0.238}$	−4.67
VA	$[+1,\ -1,\ +1,-1]$	−0.594	0.225	$^{+0.028}_{-0.120}$	$^{+0.227}_{-0.255}$	−1.21
		0.676	0.200	$^{+0.078}_{-0.019}$	$^{+0.215}_{-0.201}$	−3.25
X1	$[+1,\ -1,\ 0,\ 0]$	0.682	0.267	$^{+0.339}_{-0.243}$	$^{+0.432}_{-0.361}$	−5.52
X2	$[+1,\ 0,\ +1,\ 0]$	0.089	0.121	$^{+0.046}_{-0.017}$	$^{+0.129}_{-0.122}$	−0.52
X3	$[+1,\ 0,\ 0,+1]$	0.158	0.108	$^{+0.009}_{-0.019}$	$^{+0.109}_{-0.110}$	−2.09
X4	$[\ 0,\ +1,\ +1,\ 0]$	−0.029	0.116	$^{+0.098}_{-0.026}$	$^{+0.151}_{-0.119}$	−0.06
X5	$[\ 0,\ +1,\ 0,+1]$	0.079	0.123	$^{+0.052}_{-0.018}$	$^{+0.133}_{-0.124}$	−0.41
X6	$[\ 0,\ 0,\ +1,-1]$	−0.786	0.274	$^{+0.192}_{-0.295}$	$^{+0.334}_{-0.402}$	−6.01

Table 1: *Relations between couplings $[\epsilon_{LL}, \epsilon_{LR}, \epsilon_{RL}, \epsilon_{RR}]$ for the considered compositeness models and the contact interaction coupling values, η^{Data}, determined from the simultaneous QCD+CI fit to the HERA inclusive data; δ_{exp}, δ_{mod} and δ_{tot}, represent the experimental, modelling and total uncertainties, respectively. Also shown is the change of the χ^2 value relative to the fit performed without the CI contribution, $\Delta\chi^2 = \chi^2_{SM+CI} - \chi^2_{SM}$. For VA model two minima in the χ^2 distribution are considered, separately for negative and for positive coupling values (see text for details).*

ZEUS

HERA $e^{\pm}p$ 1994-2007 data

Model	Coupling Structure	Coupling fit results (TeV^{-2})				$\Delta\chi^2$
		$\eta_{\mathrm{LQ}}^{\mathrm{Data}}$	δ_{exp}	δ_{mod}	δ_{tot}	
$S_\circ^L$	$a_{LL}^{eu} = +\frac{1}{2}$	-0.258	0.196	$^{+0.034}_{-0.036}$	$^{+0.199}_{-0.199}$	-1.56
$S_\circ^R$	$a_{RR}^{eu} = +\frac{1}{2}$	0.533	0.331	$^{+0.034}_{-0.061}$	$^{+0.332}_{-0.336}$	-2.53
$\tilde{S}_\circ^R$	$a_{RR}^{ed} = +\frac{1}{2}$	-2.561	1.115	$^{+0.323}_{-0.221}$	$^{+1.161}_{-1.137}$	-3.98
$S_{1/2}^L$	$a_{LR}^{eu} = -\frac{1}{2}$	0.054	0.341	$^{+0.075}_{-0.280}$	$^{+0.349}_{-0.441}$	-0.02
$S_{1/2}^R$	$a_{RL}^{ed} = a_{RL}^{eu} = -\frac{1}{2}$	0.112	0.491	$^{+0.118}_{-0.412}$	$^{+0.505}_{-0.641}$	-0.05
$\tilde{S}_{1/2}^L$	$a_{LR}^{ed} = -\frac{1}{2}$	0.463	1.371	$^{+0.925}_{-0.264}$	$^{+1.654}_{-1.396}$	-0.10
S_1^L	$a_{LL}^{ed} = +1,\ a_{LL}^{eu} = +\frac{1}{2}$	0.970	0.203	$^{+0.043}_{-0.337}$	$^{+0.207}_{-0.393}$	-11.10
$V_\circ^L$	$a_{LL}^{ed} = -1$	-0.326	0.116	$^{+0.030}_{-0.101}$	$^{+0.120}_{-0.154}$	-6.17
$V_\circ^R$	$a_{RR}^{ed} = -1$	1.280	0.558	$^{+0.111}_{-0.163}$	$^{+0.568}_{-0.581}$	-3.98
$\tilde{V}_\circ^R$	$a_{RR}^{eu} = -1$	-0.267	0.165	$^{+0.030}_{-0.017}$	$^{+0.168}_{-0.166}$	-2.53
$V_{1/2}^L$	$a_{LR}^{ed} = +1$	-0.231	0.685	$^{+0.132}_{-0.460}$	$^{+0.698}_{-0.825}$	-0.10
$V_{1/2}^R$	$a_{RL}^{ed} = a_{RL}^{eu} = +1$	-0.056	0.246	$^{+0.206}_{-0.059}$	$^{+0.320}_{-0.253}$	-0.05
$\tilde{V}_{1/2}^L$	$a_{LR}^{eu} = +1$	-0.027	0.171	$^{+0.139}_{-0.038}$	$^{+0.220}_{-0.175}$	-0.02
V_1^L	$a_{LL}^{ed} = -1,\ a_{LL}^{eu} = -2$	0.029	0.077	$^{+0.015}_{-0.013}$	$^{+0.079}_{-0.079}$	-0.14

Table 2: *Coefficients a_{ij}^{eq} defining the effective leptoquark couplings in the contact-interaction limit, $M_{LQ} \gg \sqrt{s}$, and the coupling values, η_{LQ}^{Data}, determined from the simultaneous QCD+CI fit to the HERA inclusive data, for different models of scalar (upper part of the table) and vector (lower part) leptoquarks.; δ_{exp}, δ_{mod} and δ_{tot}, represent the experimental, modelling and total uncertainties, respectively. Also shown is the change of the χ^2 value relative to the fit performed without the LQ contribution, $\Delta\chi^2 = \chi^2_{SM+LQ} - \chi^2_{SM}$.*

Variation	Standard Value	Lower Limit	Upper Limit
Q^2_{min} [GeV^2]	3.5	2.5	5.0
charm mass parameter M_c [GeV]	1.47	1.41	1.53
beauty mass parameter M_b [GeV]	4.5	4.25	4.75
sea strange fraction f_s	0.4	0.3	0.5
starting scale μ_{f_0} [GeV]	1.9	1.6	2.2

Table 3: *Input parameters for the fit and the variations considered to evaluate model and parameterisation (μ_{f_0}) uncertainties.*

ZEUS

HERA $e^{\pm}p$ 1994-2007 data

Model	η^{Data}	p_{SM}	95% C.L. coupling limits (TeV^{-2})						95% C.L. mass scale limits (TeV)			
			Measured (exp)		Measured (exp+mod)		Expected		Measured (exp+mod)		Expected	
	(TeV^{-2})	(%)	η^-	η^+	η^-	η^+	η^-	η^+	Λ^-	Λ^+	Λ^-	Λ^+
LL	0.305	7.0	−0.033	0.610	−0.077	0.616	−0.367	0.319	12.8	4.5	5.9	6.3
RR	0.338	5.9	−0.017	0.649	−0.058	0.656	−0.390	0.337	14.7	4.4	5.7	6.1
LR	−0.084	34	−0.514	0.250	−0.565	0.413	−0.388	0.313	4.7	5.5	5.7	6.3
RL	−0.040	42	−0.464	0.299	−0.503	0.444	−0.397	0.302	5.0	5.3	5.6	6.5
VV	0.041	25	−0.058	0.135	−0.065	0.155	−0.101	0.097	13.9	9.0	11.2	11.4
AA	0.326	0.6		0.530	−0.051	0.700	−0.200	0.207	15.7	4.2	7.9	7.8
VA	−0.594 0.676	5.8 2.5	−0.888	0.947	−0.969	0.997	-0.723	0.719	3.6	3.5	4.2	4.2
X1	0.682	0.4		1.020		1.230	−0.435	0.418		3.2	5.4	5.5
X2	0.089	24	−0.113	0.269	−0.125	0.310	−0.206	0.184	10.4	6.4	7.8	8.3
X3	0.158	7.3	−0.018	0.320	−0.039	0.324	−0.183	0.166	17.9	6.2	8.3	8.7
X4	−0.029	39	−0.230	0.144	−0.243	0.223	−0.194	0.170	7.2	7.5	8.0	8.6
X5	0.079	27	−0.129	0.263	−0.138	0.303	−0.212	0.188	9.5	6.4	7.7	7.7
X6	−0.786	0.3	−1.130		−1.310		−0.454	0.415	3.1		5.3	5.5

Table 4: *Contact interaction coupling values determined from the fit to the HERA inclusive data, η^{Data}, and probabilities to obtain larger absolute coupling values from the fit to the Standard Model replicas, p_{SM}, for the considered CI models. Also shown are the 95% C.L. limits on the contact interaction couplings obtained from the presented analysis without (exp) and with (exp+mod) taking into account model and parameterisation variations in the fitting procedure. Lower and upper coupling limits, η^- and η^+, are calculated separately for negative and positive coupling values. The upper 95% C.L. limits on the compositeness scale, Λ^+ and Λ^-, correspond to the scenarios with positive and negative coupling values, respectively. The same coupling structure applies to all quarks. Only positive coupling values are allowed at 95% C.L. for the X1 model, while for the X6 model only negative coupling values are allowed. For VA model, fit range is restricted to negative or positive couplings, for lower and upper limit calculation, respectively (see text for details).*

ZEUS

HERA $e^{\pm}p$ 1994-2007 data

Model	Coupling Structure	η_{LQ}^{Data} (TeV^{-2})	p_{SM} (%)	λ_{LQ}/M_{LQ} 95% C.L. limits (TeV^{-1}) Measured (exp)	Measured (exp+mod)	Expected
$S_{\circ}^{L}$	$a_{LL}^{eu} = +\frac{1}{2}$	-0.258	9.0	0.25	0.28	0.56
$S_{\circ}^{R}$	$a_{RR}^{eu} = +\frac{1}{2}$	0.533	5.5	1.02	1.03	0.72
$\tilde{S}_{\circ}^{R}$	$a_{RR}^{ed} = +\frac{1}{2}$	-2.561	1.8			1.71
$S_{1/2}^{L}$	$a_{LR}^{eu} = -\frac{1}{2}$	0.054	43	0.80	0.83	0.76
$S_{1/2}^{R}$	$a_{RL}^{ed} = a_{RL}^{eu} = -\frac{1}{2}$	0.112	39	0.99	1.04	0.92
$\tilde{S}_{1/2}^{L}$	$a_{LR}^{ed} = -\frac{1}{2}$	0.464	38	1.51	1.66	1.39
S_{1}^{L}	$a_{LL}^{ed} = +1,\ a_{LL}^{eu} = +\frac{1}{2}$	0.974	< 0.01	1.16	1.18	0.62
$V_{\circ}^{L}$	$a_{LL}^{ed} = -1$	-0.325	0.5			0.44
$V_{\circ}^{R}$	$a_{RR}^{ed} = -1$	1.280	1.8	1.44	1.47	0.99
$\tilde{V}_{\circ}^{R}$	$a_{RR}^{eu} = -1$	-0.267	5.5	0.06	0.18	0.53
$V_{1/2}^{L}$	$a_{LR}^{ed} = +1$	-0.231	38	1.12	1.19	1.29
$V_{1/2}^{R}$	$a_{RL}^{ed} = a_{RL}^{eu} = +1$	-0.056	39	0.55	0.67	0.57
$\tilde{V}_{1/2}^{L}$	$a_{LR}^{eu} = +1$	-0.027	43	0.47	0.59	0.49
V_{1}^{L}	$a_{LL}^{ed} = -1,\ a_{LL}^{eu} = -2$	0.029	32	0.39	0.41	0.25

Table 5: *Coefficients a_{ij}^{eq} defining the effective leptoquark couplings in the contact-interaction limit, $M_{LQ} \gg \sqrt{s}$, coupling values determined from the fit to the HERA inclusive data, η_{LQ}^{Data}, and the upper limits on the Yukawa coupling to the leptoquark mass ratio, λ_{LQ}/M_{LQ}, for different models of scalar (upper part of the table) and vector (lower part) leptoquarks. Limits calculated without (exp) and with (exp+mod) taking into account modelling uncertainties of the fitting procedure are compared with the expected limits from the presented analysis. For $\tilde{S}_{\circ}^{R}$ and $V_{\circ}^{L}$ models limit values are not given as all positive coupling values are excluded on 95% C.L.*

ZEUS

Coupling structure		95% C.L. limits (TeV)					
		HERA		ATLAS		CMS	
Model	$[\epsilon_{LL},\epsilon_{LR},\epsilon_{RL},\epsilon_{RR}]$	Λ^-	Λ^+	Λ^-	Λ^+	Λ^-	Λ^+
LL	$[+1, \ 0, \ 0, \ 0\ ]$	12.8	4.5	24	37	13.5	18.3
RR	$[\ 0, \ 0, \ 0, +1\ ]$	14.7	4.4	26	33		
LR	$[\ 0, +1, \ 0, \ 0\ ]$	4.7	5.5	26	33		
RL	$[\ 0, \ 0, +1, \ 0\ ]$	5.0	5.3	26	33		

Table 6: *Comparison of the* 95% *C.L. limits on the compositeness scale,* Λ*, obtained from the ZEUS analysis of the HERA inclusive data with results on eeqq contact interactions from the ATLAS Collaboration analysis of the 13 TeV LHC data [15] and from the CMS Collaboration using the full 8-TeV dataset [14]. For ATLAS experiment, limits obtained with the assumed uniform positive prior in* $1/\Lambda^2$ *are shown.*

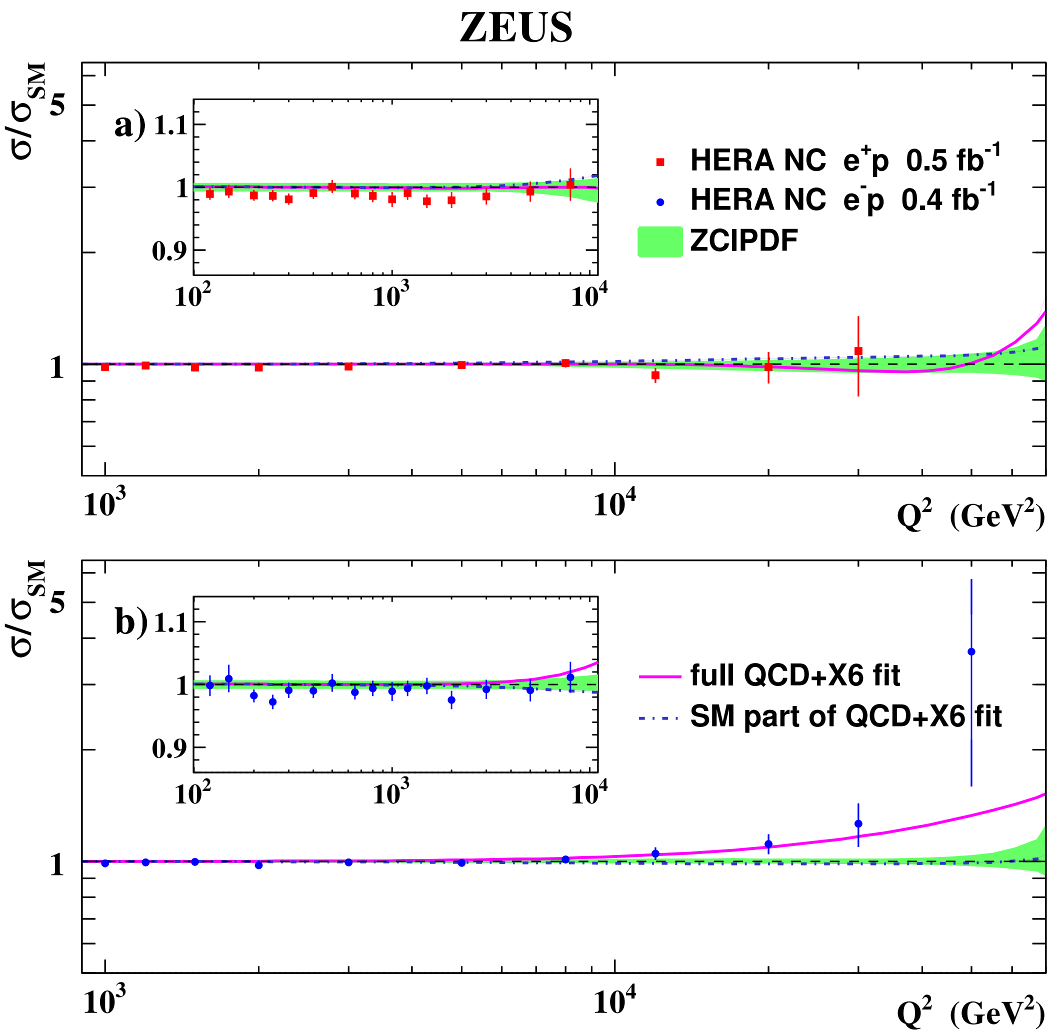

Figure 1: *Result of the simultaneous QCD+CI fit to the HERA inclusive data, for the X6 contact interaction model, compared to the combined HERA (a) e^+p and (b) e^-p NC DIS data, relative to the SM expectations based on the QCD fit without the CI contribution (ZCIPDF). The bands represent the total uncertainty of the SM expectations. Also shown is the SM contribution to the cross section, resulting from the combined fit.*

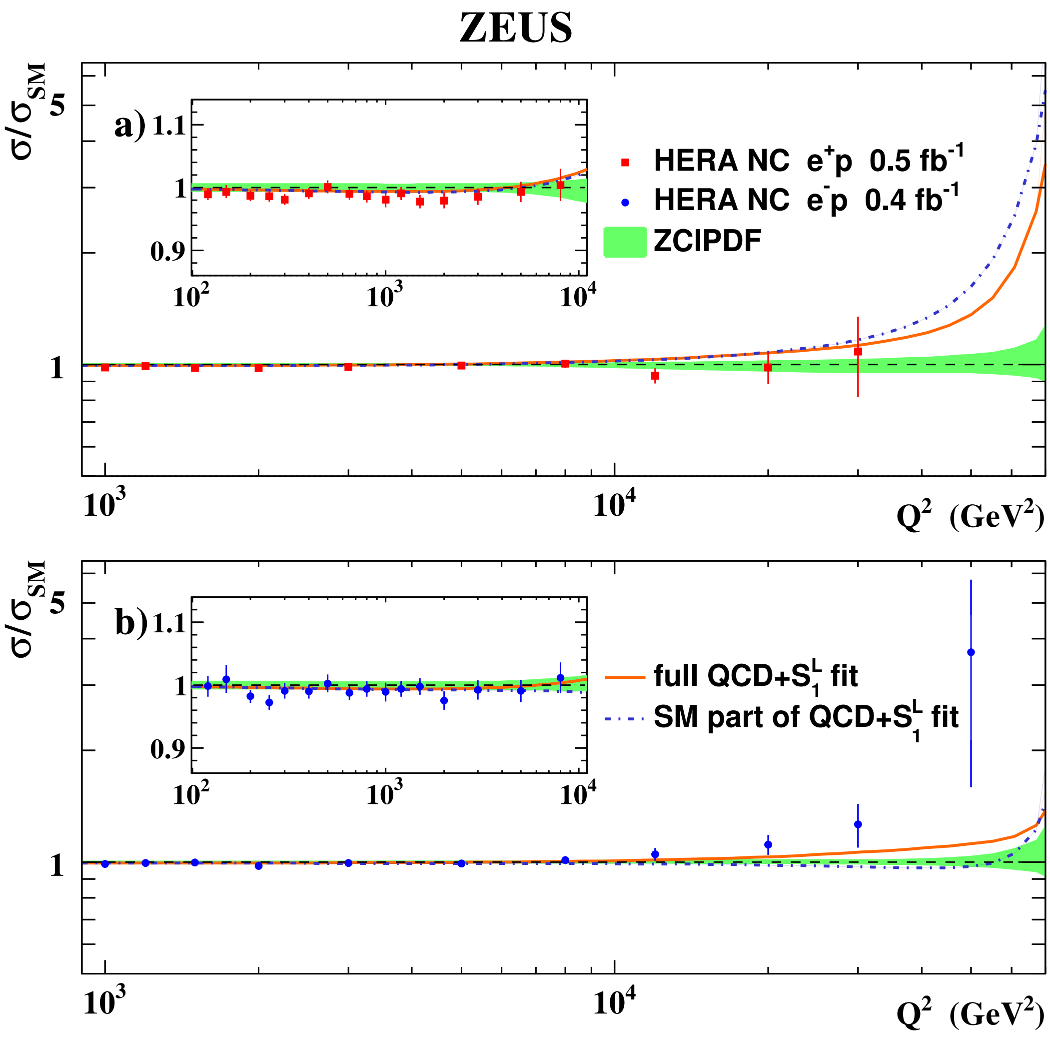

Figure 2: *Result of the simultaneous QCD+LQ fit to the HERA inclusive data, for the S_1^L leptoquark model in the contact interaction limit, $M_{LQ} \gg \sqrt{s}$, compared to the combined HERA (a) e^+p and (b) e^-p NC DIS data, relative to the SM expectations based on the QCD fit without the CI contribution (ZCIPDF). The bands represent the total uncertainty of the SM expectations. Also shown is the SM contribution to the cross section, resulting from the combined fit.*

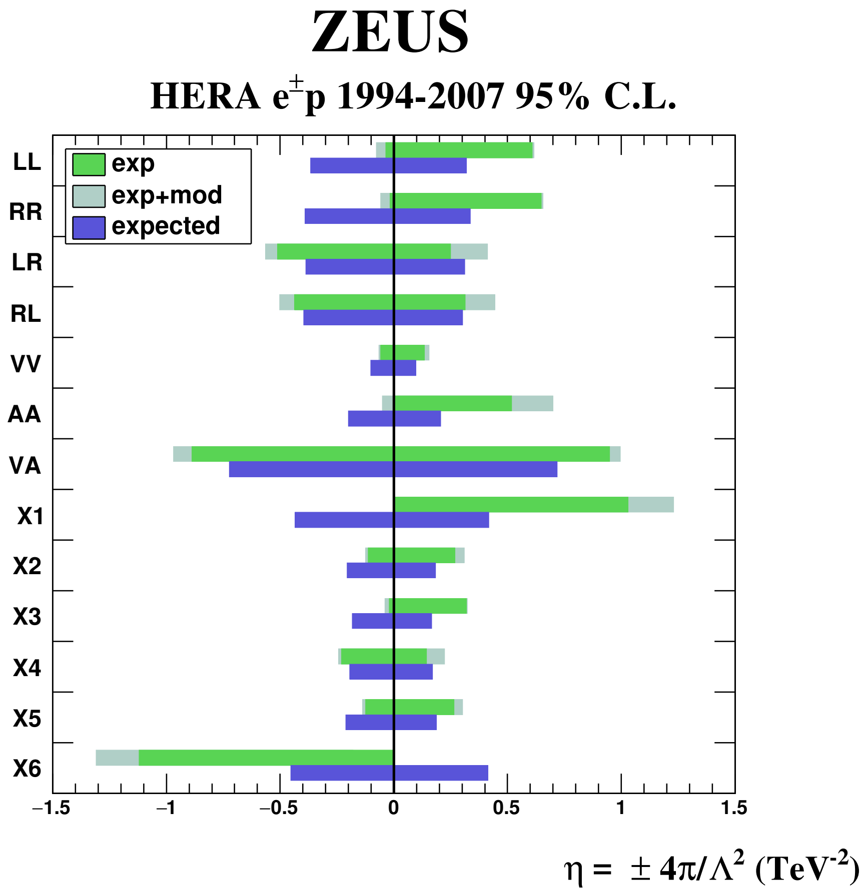

Figure 3: *Limits on the CI coupling strength, $\eta = \pm 4\pi/\Lambda^2$, for CI scenarios studied in this paper, evaluated at 95% C.L. Compared are the limits calculated without (dark green horizontal bars) and with (light green bars) modelling uncertainties taken into account, and the expected limits (blue bars). Limits are calculated separately for positive and negative coupling values (see text for details).*

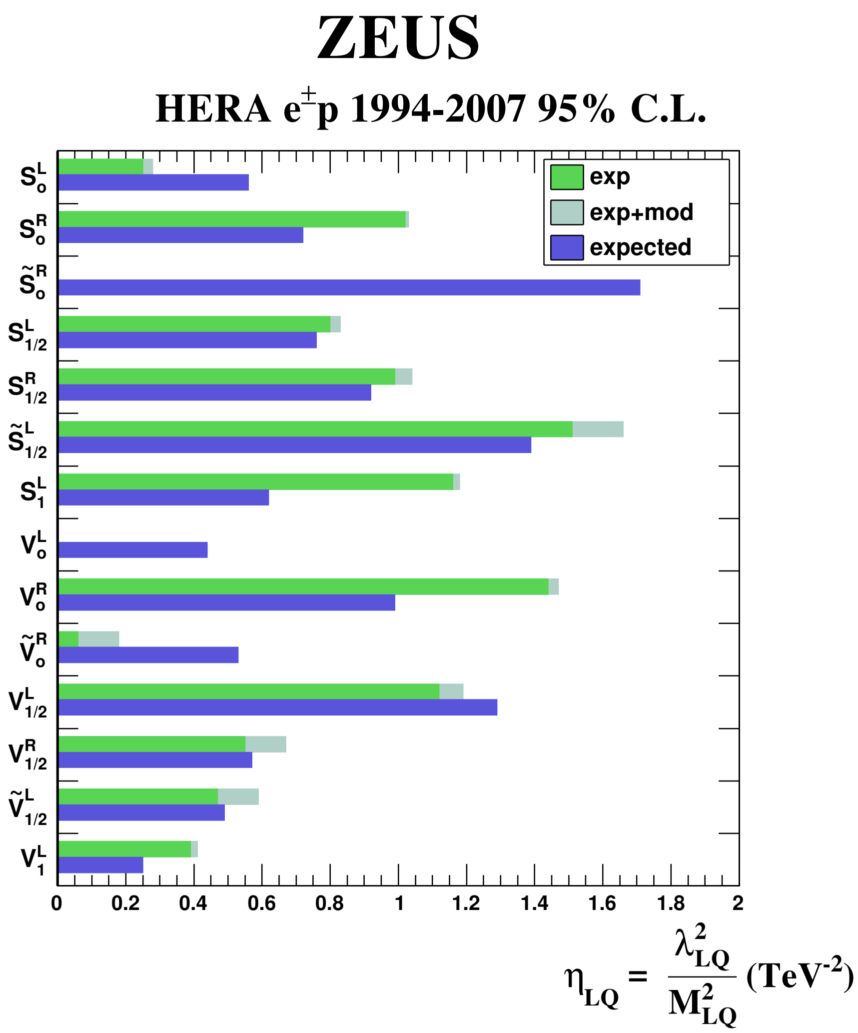

Figure 4: *Upper 95% C.L. limits on the LQ coupling strength, $\eta_{LQ} = \lambda_{LQ}^2/M_{LQ}^2$, for leptoquark scenarios studied in this paper. Compared are the limits calculated without (dark green horizontal bars) and with (light green bars) modelling uncertainties taken into account, and the expected limits (blue bars).*

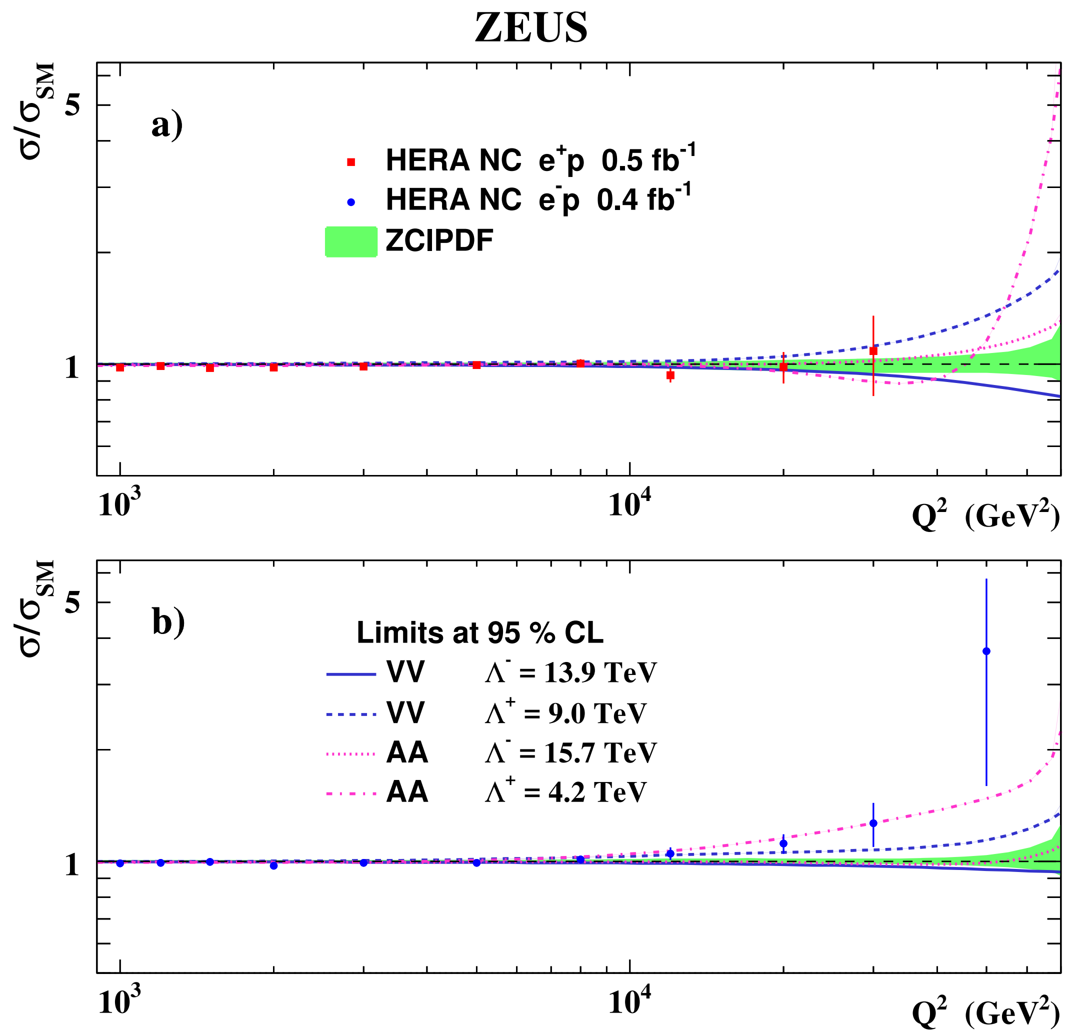

Figure 5: *Combined HERA (a) e^+p and (b) e^-p NC DIS data, relative to the SM expectations based on the PDF fit to the HERA inclusive data, compared to the 95% C.L. limits on the effective mass scale in the VV and AA contact-interaction models, for positive (Λ^+) and negative (Λ^-) couplings (same four models are shown on both plots). The bands represent the total uncertainty of the QCD fit predictions.*

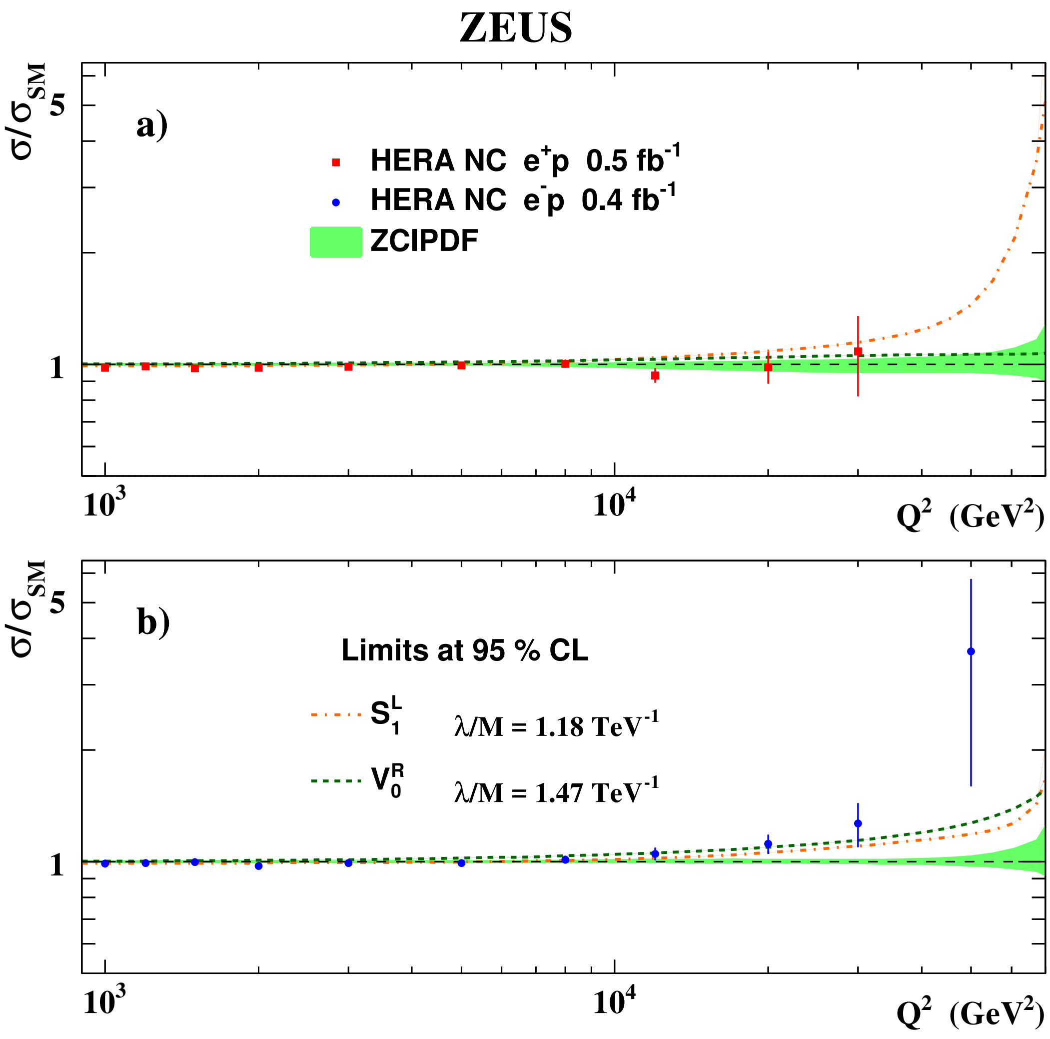

Figure 6: *Combined HERA (a) e^+p and (b) e^-p NC DIS data, relative to the SM expectations based on the PDF fit to the HERA inclusive data, compared to the limits on the ratio of the leptoquark Yukawa coupling to the leptoquark mass, λ/M, corresponding to the 95% C.L. limit on the LQ coupling value resulting from the presented analysis, for the S_1^L and $V_\circ^R$ leptoquarks (same two models are shown on both plots). The bands represent the total uncertainty of the QCD fit predictions.*